**Paper:**

# Time-Series Data Analysis Using Sliding Window Based SVD for Motion Evaluation

**Yinlai Jiang**[*1], **Isao Hayashi**[*2], **Shuoyu Wang**[*3], **and Kenji Ishida**[*4]

[*1]The University of Electro-Communications
Chofu, Tokyo 182-8585, Japan
E-mail: jiang@hi.mce.uec.ac.jp
[*2]Kansai University
Takatsuki, Osaka 569-1095, Japan
E-mail: ihaya@cbii.kutc.kansai-u.ac.jp
[*3]Kochi University of Technology
Kami, Kochi 782-8502, Japan
E-mail: wang.shuoyu@kochi-tech.ac.jp
[*4]Kurihara Central Hospital
Kurihara, Miyagi 987-2205, Japan
E-mail: kenji-i@kam.or.jp

[Received December 30, 2016; accepted August 31, 2017]

**A method based on singular value decomposition (SVD) is proposed for extracting features from motion time-series data observed with various sensing systems. Matrices consisting of the sliding window (SW) subsets of time-series data are decomposed, yielding singular vectors as the patterns of the motion, and the singular values as a scalar, by which the corresponding singular vectors describe the matrices. The sliding window based singular value decomposition was applied to analyze acceleration during walking. Three levels of walking difficulty were simulated by restricting the right knee joint in the measurement. The accelerations of the middles of the shanks and the back of the waist were measured and normalized before the SW-SVD was performed.The results showed that the first singular values inferred from the acceleration data of the restricted side (the right shank) significantly related to the increase of the restriction among all the subjects while there were no common trends in the singular values of the left shank and the waist. The SW-SVD was suggested to be a reliable method to evaluate walking disability. Furthermore, a 2D visualization tool is proposed to provide intuitive information about walking difficulty which can be used in walking rehabilitation to monitor recovery.**

**Keywords:** singular value decomposition, time-series data analysis, sliding window, motion analysis, walking difficulty evaluation

## 1. Introduction

Body motion contains vast information such as communicative message [1, 2], motion capability [3, 4], skill level [5], even the characteristic and the identity of a person [6, 7]. The motions performed by the human musculoskeletal system are learned, programed and generated by the nervous system including the cerebral cortex, the cerebellum, the brain stem and the spinal cord. The dexterity of body motion therefore embodies the human knowledge related to body control. The embodied knowledge, or tacit knowledge, internalized in the body is a native human endowment that plays an important role in acquiring and performing skills. Neurophysiological study on embodied knowledge by Kawato et al. proposed a cerebellar computational model, called an internal model, which argued that the inverse model with feedback and feed forward control is useful in modeling motor control [8, 9]. Hall et al. further suggest that this intrinsic rhythmicity of around 3 Hz reflects an underlying organization of motor cortical circuits engaged in feedback control of movement [10].

Embodied knowledge has also been studied from the viewpoint of the kinesiology by using the kinematic information of motion, such as trajectory [5], speed [11], and acceleration [12, 13]. Analysis of the time-series data is usually required to extract features from large-scale and multidimensional kinematic information [14]. Various methods, such as Hidden Markov model (HMM) [15, 16], Dynamic time warping (DTW) [17], artificial neural network (ANN) [18], principal component analysis (PCA) [19, 20], and correlation coefficient (CC) [21] have been utilized to analyze time-series data of physical movement.

Recently, Singular Value Decomposition (SVD) [22, 23] has shown its effectiveness in time-series data analysis. Nakanishi et al. studied the coordinative structures in human behavior by constructing multiple alignments from the time-series data and detecting motion change points with the SVD [24]. Cavallo et al. segmented time-series data with the SVD for the real-time classification of manipulation tasks [25]. In previous studies [26, 27], authors have proposed a method based on the SVD to extract features from time-series data. The matrix defined from the time-series data are decomposed into singular vectors and singular values. The left singular vectors extracted from time series of trajectory data was applied to a hand gesture recognition experiment and the experiment results confirmed that the proposed method led to a high recognition rate than PCA and correlation efficiency (CE) [26]. The singular values extracted from time series of acceleration data was suggested to be a reliable criterion to evaluate walking disability [27].

This study focuses on the evaluation of motion capability based on time-series analysis using the SVD. Although the previous study [27] has shown the effectiveness of singular values in the evaluation, data preprocessing, such as the segmentation of the motion cycles to guarantee each column of the matrix to be composed of one cycle, and data alignment by interpolation and deletion to make the cycle length the same, are required. These preprocessing increases the complexity of calculation, and thus decreases the applicability in practical use. The performance of the method may also be affected by the implementation of segmentation and alignment since different algorithms may lead to different results.

A new method free of segmentation and alignment is therefore proposed in this paper to extract motion features using Sliding Window based SVD (SW-SVD). Section 2 describes the SW-SVD. Section 3 validates the SW-SVD with a walking difficulty evaluation experiment. The accelerations of walking were measured for three levels of difficulty and the singular values extracted from the acceleration data are investigated as a criterion to evaluate walking difficulty. The results are compared with those of the previous study [27]. Section 4 introduces a visualization tool for future use in walking rehabilitation to show the singular values in a human-friendly manner. Discussions on the experimental results and the visualization tool are given in Section 5. Finally, Section 6 concludes the paper and discusses the future work.

## 2. Sliding Window Based SVD

### 2.1. Standard SVD

The SVD is a factorization of a rectangular real or complex matrix with many applications in signal processing and statistics [22, 23]. Suppose $M$ is an $m$-by-$n$ matrix, then a factorization of $M$ is

$$M = U\Sigma V^T \quad \quad (1)$$

where $U = (u_1, u_2, \ldots, u_m)$ is a unitary matrix with $u_1, u_2, \ldots, u_m$ being the left singular vectors of $M$, $V^T = (v_1, v_2, \ldots, v_n)^T$ is a unitary matrix with $v_1, v_2, \ldots, v_n$ being the right singular vectors of $M$, and the matrix $\Sigma$ is an $m$-by-$n$ diagonal matrix with nonnegative real singular values on the diagonal.

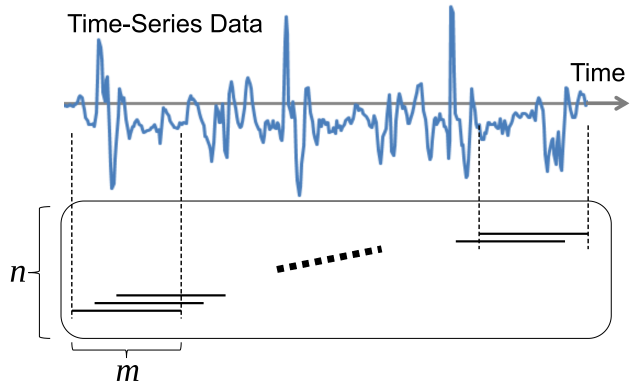


**Fig. 1.** Design of matrix using whole time-series. $m$ is the length of the segments and $n$ is the number of segments.

Denote the singular values as $\sigma_1, \sigma_2, \ldots, \sigma_L$ in the decreasing order of magnitude ($\sigma_1 \geq \sigma_2 \geq \cdots \geq \sigma_L \geq 0$). Set $d = rank(M)$, we usually have $d = L = \min\{m, n\}$ when $M$ is composed of time-series data measured in real-life. In this notation, $M$ can be written as

$$M = \sigma_1 u_1 v_1 + \sigma_1 u_1 v_1 + \cdots + \sigma_d u_d v_d \quad \quad (2)$$

This equation shows that the collection $(\sigma_i, u_i, v_i)$ can be considered as a component of $M$ with $u_i$ and $v_i$ representing the pattern of $M$ and $\sigma_i$ showing how representative the pattern is. Since $v_i = M^T u_i / \sigma_i$ according to the calculation of the SVD, either of $u_i$ and $v_i$ is utilized in analysis.

### 2.2. Feature Extraction from Matrix of Whole Time-Series

In the previous studies [26, 27], we have proposed a feature extraction method using the SVD by composing the matrix $M$ with the whole time-series data of measurement. The design of $M$ is shown in **Fig. 1**. $n$ segments each with $m$ data are extracted at certain intervals to compose the $m$-by-$n$ matrix $M$ for the SVD.

Since the singular vectors represent the characteristics of $M$ that consists of the time-series measured, we applied the left singular vectors to a hand gesture recognition experiment in which 5 hand gestures were recognized according to the singular vectors decomposed from the 3D trajectory of the hand motions. A higher recognition rate was obtained with the proposed method than those with PCA and CE [26]. On the other hand, the magnitude of the singular values may indicate the stability of the motion since the singular values shows the representativeness of the patterns in the singular vectors. We thus investigated the possibility of using the singular values from walking acceleration data as a reliable criterion to evaluate walking ability. The singular values of the left and shanks showed decreasing trend with the increase of walking difficulty [27].

The previous studies have shown the effectiveness of SVD in feature extraction from time-series data. However, issues remained concerning data preprocessing during the preparation of matrix $M$. To guarantee the perfor-

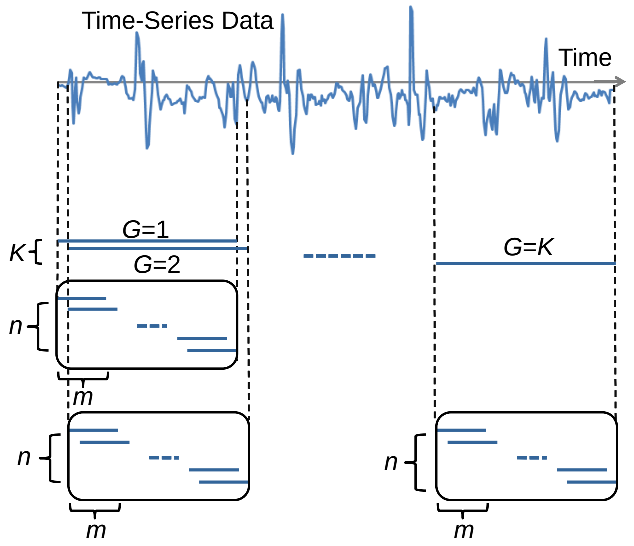


**Fig. 2.** Design of matrix using sliding window subsets. $K$ is the number of subsets, $m$ is the length of the segments, and $n$ is the number of segments in a subset.

mance, the segmentation of the motion cycles and alignment by interpolation and deletion to make the cycle length the same are required. These issues need to be solved to simplify calculation and ensure the performance not affected by the implementation of segmentation and alignment.

### 2.3. Feature Extraction from Matrix of Sliding Window Subsets of Time-Series

To exclude data preprocessing from the calculation while ensuring the performance of feature extraction, we propose to compose the matrix $M$ with sliding window subsets rather than the whole time series.

Suppose that $w$ points $(P_1, P_2, \ldots, P_w)$ on the body are measured while a motion is performed. The time series data on each point are divided into $K$ subsets by sliding windows (**Fig. 2**). On point $P_i$, the measured data series of the $G$-th subset is denoted as $\tau^{i,G}$. The data series of $\tau^{i,G}$ consists of three-dimensional data $(X^{i,G}, Y^{i,G}, Z^{i,G})$. From this time-series data $\tau^{i,G} = (X^{i,G}, Y^{i,G}, Z^{i,G})$, $n$ vectors by $m$ data sampling are extracted by overlapping and the matrices $M_X^{i,G}, M_Y^{i,G}$, and $M_Z^{i,G}$ are constructed as a collective of the measurement data on the $X, Y$, and $Z$ coordinates of the motion, respectively. **Fig. 2** shows a design for constructing the matrix $M_X^{i,G}$ that is a Hankel matrix. The matrices $M_X^{i,G}, M_Y^{i,G}$, and $M_Z^{i,G}$ are described as follows:

$$M_X^{i,G} = (X_1^{i,G}, X_2^{i,G}, \ldots, X_n^{i,G})^T \quad \ldots \ldots \ldots \quad (3)$$

$$M_Y^{i,G} = (Y_1^{i,G}, Y_2^{i,G}, \ldots, Y_n^{i,G})^T \quad \ldots \ldots \ldots \quad (4)$$

$$M_Z^{i,G} = (Z_1^{i,G}, Z_2^{i,G}, \ldots, Z_n^{i,G})^T \quad \ldots \ldots \ldots \quad (5)$$

where $X_p^{i,G} = (x_{p,1}^{i,G}, x_{p,2}^{i,G}, \ldots, x_{p,m}^{i,G})$, $p = 1, 2, \ldots, n$, and $x$ is a datum on the $X$ coordinate. $Y_p^{i,G}$ and $Z_p^{i,G}$ are defined in the same way.

Suppose $M_k^{i,G}$, $k = \{X, Y, Z\}$ is an $m$-by-$n$ matrix as the general format of $M_X^{i,G}, M_Y^{i,G}, M_Z^{i,G}$. The SVD of the matrix $M_k^{i,G}$ is

$$M_k^{i,G} = U_k^{i,G} \Sigma_k^{i,G} \{V_k^{i,G}\}^T \quad \ldots \ldots \ldots \ldots \quad (6)$$

where $U_k^{i,G} = (u_{1,k}^{i,G}, u_{2,k}^{i,G}, \ldots, u_{m,k}^{i,G})$ is an $m$-by-$m$ unitary matrix, $\{V_k^{i,G}\}^T$ denotes the conjugate transpose of $V_k^{i,G} = (v_{1,k}^{i,G}, v_{2,k}^{i,G}, \ldots, v_{n,k}^{i,G})$ which is an $n$-by-$n$ unitary matrix, and the matrix $\Sigma_k^{i,G}$ is an $m$-by-$n$ diagonal matrix. The diagonal entries of $\Sigma_k^{i,G}$ are the singular values of $M_k^{i,G}$. The matrix $U_k^{i,G}$ contains the left singular vectors of $M_k^{i,G}$ and the matrix $V_k^{i,G}$ contains the right singular vectors of $M_k^{i,G}$. A singular vector expresses the characteristic of the whole time-series data better if its corresponding singular value is larger. That is, the greater the singular value is, the more dominant the corresponding pattern is.

Choose the left singular vectors as the pattern. Suppose that the number of left singular vectors to be considered is $l$, and the element number of the $j$ th left singular vector is $q$. Let us denote the couples of the singular values and the left singular vector as

$$H_G = ((\sigma_{1,X}^{i,G}, u_{1,X}^{i,G}), (\sigma_{2,X}^{i,G}, u_{2,X}^{i,G}), \ldots, (\sigma_{l,X}^{i,G}, u_{l,X}^{i,G})) \quad (7)$$

for $u_{j,X}^{i,G} = (\hat{u}_{1j,X}^{i,G}, \hat{u}_{2j,X}^{i,G}, \ldots, \hat{u}_{hj,X}^{i,G}, \ldots, \hat{u}_{qj,X}^{i,G})$ in the descending order of the singular values, where $\hat{u}_{hj,X}^{i,G}$ is the $h$ th element of the $j$-th left singular vector $u_{j,X}^{i,G}$. $\sigma_{1,k}^{i,1}$ of $H_1$, for example, is the first (and the biggest) singular value of the first subset from the $k$ coordinate of time-series data measured on measurement point $i$. The pair $(\sigma_{1,X}^{i,G}, u_{1,X}^{i,G})$ possesses the most important feature of the $G$-th subset

Since the Hankel matrix is designed by overlapping the extracted data from the whole time-series data by sliding window, preprocessing of segmentation and alignment, is not required. The SW-SVD is not constrained by the length of the whole data. The difference between PCA and our method is that PCA generally analyzes the matrix composed of the deviation of each datum from the empirical mean and does not allow overlap of the measurement data.

## 3. Walking Ability Evaluation Using Singular Values

Kinesiological studies using wireless sensors draws increasing attention with the dissemination of portable devices such as tablets and smart phones. Especially in the field of healthcare, the development of convenient ways to monitor daily health status and predict disorder has accomplished many achievements [28, 29].

We focus attention on the walking ability assessment during the process of walking rehabilitation. Clinical measurement of walking ability are mainly based on inspection of the physical therapist, sometimes with the help of muscle strength measurement, X-ray examina-

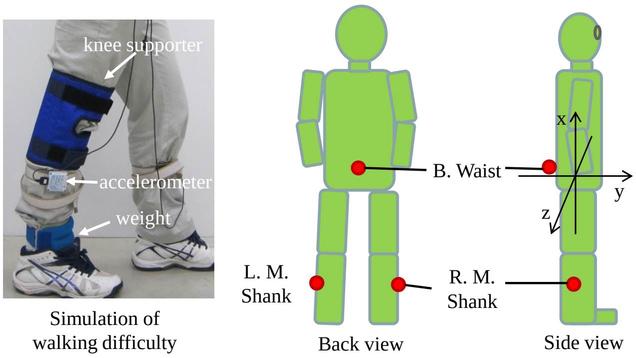


**Fig. 3.** Experiment settings.

tion, ground reaction force, 3D motion analysis, acceleration analysis, gait and stride analysis, or electromyography (EMG) and so on. Objective measurements and correct interpretation of the measurement results can have a substantial impact on the recovery since it is important to track the recovery and thus to design the proper rehabilitation program according to the condition of the patient. Furthermore, a convenient assessment method is desired for those who rehabilitate and exercise at their homes, thus they can know their status anytime by themselves.

Since the singular values indicate the strength of the corresponding singular vectors that represent the characteristics of the Hankel matrix, the matrix composed of time-series data of stable motions should have relatively large singular values. The singular values therefore can be considered as an index to evaluate the stability of motion. In this section, the singular values from walking acceleration data are applied to evaluate the levels of walking disability. Compact, wearable, and convenient accelerometers have been widely used to monitor body movements, including gait, sit-to-stand transfers, postural sway, and falls. They have been used in clinician to evaluate physical activity levels [12], to identify and classify movements [30, 31], and to analyze gait pattern in diseases [32, 33].

### 3.1. Walking Acceleration Measurement

Six healthy subjects aged 21-31 yr (mean 26 yr) participated in the experiment. All subjects were fully informed about the procedures, risk, and benefits of the study as well as the specifications of the devices, and written informed consents were obtained from all the subjects before the study. The study was carried out in accordance with the principles outlined in the Declaration of Helsinki. The experimental protocol was approved by the ethics board of Kochi University of Technology.

In order to measure the acceleration of different walking abilities, we simulated walking difficulty by restricting the right knee joint with knee supporters and weight bands (**Fig. 3**). The knee supporter, with plastic plates inside, wrapped around the knee joint decreases the range of movement (ROM) of the knee joint, and the weight band bound around the ankle joint can simulate the weakness in muscle strength. The simulation is very important in testing our method since it does not endanger the safety of the disabled during the development phase of the method. Furthermore, the simulation allows us to create different levels of the same symptom to validate the method, which is difficult by recruiting patients. In medical practice, the walking disabilities are quite various, common trends are hard to obtain by a small number of subjects. The experiment in this study only simulated one aspect of walking difficulties to verify the proposed SW-SVD. The similar methods to simulate walking difficulty were also used in other studies [34, 35].

Two levels of walking difficulty were simulated by two levels of constraint. One knee supporter and one weight band (1 kg) simulated the weak constraint, and two knee supporters and two weight bands (2 kg) simulated the strong constraint. In total, three statuses (Normal without constraint, Weak, and Strong) were measured.

The subjects were instructed to walk for approximately 4 m along a straight line. The experiment was carried out in the order of Normal, Weak, and Strong. For each status, each subject walked four times.

The acceleration is measured by 3 wearable wireless 3-axis accelerometers (Motion Recorder MVP-RF8, MicroStone Corporation, Nagano, Japan) fixed to the back of the waist (B. Waist), the midpoint of the right shank (R. M. Shank), and the midpoint of the left shank (L. M. Shank), as shown in **Fig. 3**. Sampling rate of the sensors was 100 Hz. The sensors' $x$-axis is up/down, $y$-axis front/back, and $z$-axis right/left when the subject standing upright. However, since the orientation of the sensors changes during walking, the coordination system changes correspondingly.

Examples of the acceleration time-series measured are shown in **Fig. 4**. **Fig. 4(a)** shows the $x$-coordinate acceleration at R. M. Shank when a subject walking in the three statuses. **Fig. 4(b)** shows the acceleration time-series at R. M. Shank when a subject walking in the status of weak. The acceleration data of one stride are shown in **Fig. 4(c)**. All the acceleration at the B. Waist, R. M. Shank, and L. M. Shank significantly fluctuated when the right foot pushed off from the floor or stepped on the floor. The acceleration fluctuation at L. M. Shank was more significant than that at R. M. Shank since the right leg was restricted by the knee supporter and the weight band. The fluctuation in the acceleration at B. Waist was the smallest among the three measurement points. This showed that the trunk of the body, especially the waist, was kept relatively stable to maintain the body balance even when the lower limbs were restricted.

### 3.2. Data Analysis Using SW-SVD

Stricter constraint leads to slower walking, and thus to affect the magnitudes of the accelerations. The effectiveness of the SW-SVD cannot be validated if the SW-SVD is performed on the raw data because the values of the singular values are affected by the magnitudes of the items in the Hankel matrix. Therefore, the time series data are

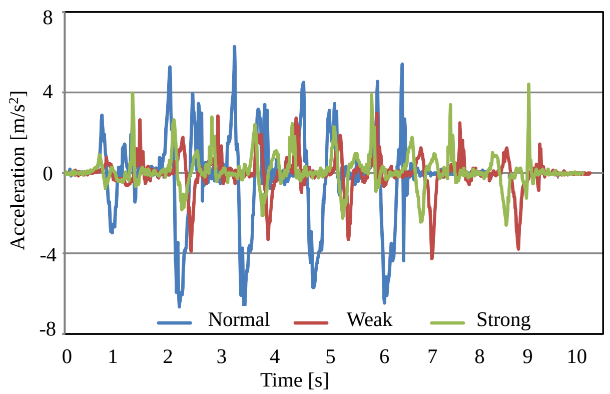

(a) Acceleration time series of the three statuses .
(x axis, R.M.Shank)

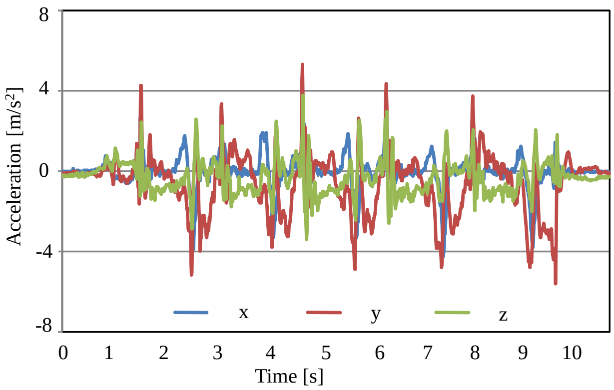

(b) Acceleration time series of R.M.Shank.

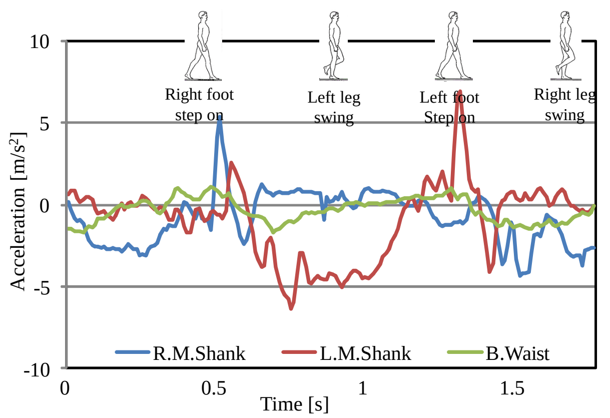

(c) Acceleration time series of the three points.
(status of Weak, x axis)

**Fig. 4.** Examples of acceleration time-series.

normalized in order to exclude the impact of the magnitudes of the acceleration. For every series of the acceleration data, the maximum acceleration $a_{\max}$ is set to 1, the minimum acceleration $a_{\min}$ to 0, and the other values $a_{nl} = (a - a_{\min})/(a_{\max} - a_{\min})$ while $a$ is the original value and $a_{nl}$ is the normalized value.

After normalization, the SW-SVD is performed on every series of acceleration data. Parameters $m$ and $n$ are very critical for the performance of SW-SVD. The selection of them depends on the periodicity of the time-series data and the desired features. As shown in **Fig. 4**, the period of on step was around 1 s during which 100 data were measured (sampling rate: 100 Hz). To investigate the relatively detailed features of walking, Hankel matrices with 10 rows and 10 columns were composed from the subsets of data, that is $n = 10$, $m = 10$. The number of subsets $K$ was determined by the total number of data in each acceleration time-series data $N$ ($K = N - m - n + 1$). The first singular values were considered in the current analysis. Thus parameter $l$ was 1. The first singular values of all the $H_G$s of a single series of acceleration were sorted in descending order. The top 50 first singular values were adopted and their mean value was considered as the criterion to evaluate the walking difficulty. There were 3 measurement points: B. Waist, R. M. Shank, L. M. Shank, each of which had 3 dimensions. Therefore, 9 groups of first singular values were calculated for each subject.

## 4. Results

The mean values of the singular values extracted from the acceleration time-series are listed in **Table 1**. $S_x$, $S_y$, and $S_z$ are the singular values of $x$, $y$, and $z$ coordinates. The singular values of the six subjects and their average at the 3 levels of walking difficulty are listed in the table. At measurement point B. Waist, no common trend among the subject was found with the 3 levels of walking difficulty (Normal, Weak, and Strong). The waist is near to the body's center of gravity and is always kept relatively stable during walking. **Fig. 4(c)** shows that the fluctuation range of the acceleration of the waist was relatively smaller to maintain the body balance. At measurement point L. M. Shank, although increasing or decreasing trends were found with the walking difficulty in some subjects, there were no consistent trends among the subjects. The constraint to the right knee also affected the gait of the left leg. However, the effect was different among the subjects due to the different biomechanics of them. At measurement point R. M. Shank, common changing trends were observed in the mean values with the increase of walking difficulty. On the $x$ and $y$ coordinates, the singular values increased with the increasing walking difficulty. On the $z$ coordinate, the singular values decreased with the increasing walking difficulty. With respect to trend of the individual subject, the $S_x$ of 5 subjects (Sub_1 to Sub_5), the $S_y$ of 4 subjects (Sub_2, Sub_3, Sub_5 and Sub_6), and the $S_z$ of 3 subjects (Sub_3, Sub_4 and Sub_6) are in the same trend with the mean values. Since R. M. Shank was located on the same side of the restricted knee, the acceleration measured by R. M. Shank most reflected the walking difficulty posed by the constraint.

A one way analysis of variance (ANOVA) was performed on the singular values at R. M. Shank to assess the significance of the difference among the three levels. ANOVA is widely used to determine whether the differences between the means of three or more groups are significant. If the P Val.$\leq$ 0.05 (significance level), the differences are considered statistically significant. The re-

**Table 1.** Means of the singular values.

| Subjects | Constraint Ambulation | B. Waist | | | R. M. Shank | | | L. M. Shank | | |
|---|---|---|---|---|---|---|---|---|---|---|
| | | $S_x$ | $S_y$ | $S_z$ | $S_x$ | $S_y$ | $S_z$ | $S_x$ | $S_y$ | $S_z$ |
| Sub_1 | Normal | 5.01 | 6.66 | 6.75 | 5.97 | 5.15 | 3.70 | 5.76 | 4.35 | 8.03 |
| | Weak | 4.89 | 7.87 | 7.57 | 4.94 | 5.05 | 3.25 | 5.27 | 4.67 | 7.81 |
| | Strong | 4.60 | 8.19 | 7.89 | 3.96 | 4.33 | 4.59 | 4.94 | 6.58 | 7.81 |
| Sub_2 | Normal | 7.21 | 8.17 | 8.43 | 7.90 | 6.47 | 4.65 | 7.84 | 6.50 | 6.78 |
| | Weak | 6.82 | 8.59 | 8.81 | 7.12 | 7.28 | 6.00 | 7.72 | 6.57 | 7.17 |
| | Strong | 6.63 | 8.72 | 9.13 | 5.13 | 7.62 | 4.74 | 8.01 | 6.37 | 6.94 |
| Sub_3 | Normal | 6.95 | 8.08 | 7.31 | 8.33 | 5.38 | 4.83 | 8.22 | 5.91 | 6.19 |
| | Weak | 7.35 | 8.66 | 7.78 | 7.73 | 6.92 | 5.77 | 7.25 | 6.10 | 6.88 |
| | Strong | 5.77 | 8.92 | 7.86 | 5.60 | 7.10 | 6.12 | 7.81 | 6.85 | 6.18 |
| Sub_4 | Normal | 5.70 | 8.52 | 7.11 | 7.02 | 4.83 | 3.74 | 7.26 | 6.98 | 7.22 |
| | Weak | 5.77 | 8.06 | 7.66 | 5.39 | 5.57 | 4.32 | 5.72 | 6.64 | 7.72 |
| | Strong | 5.24 | 8.62 | 7.11 | 4.54 | 5.50 | 4.58 | 5.34 | 5.91 | 7.34 |
| Sub_5 | Normal | 6.36 | 8.07 | 6.66 | 6.99 | 6.03 | 5.53 | 6.01 | 5.89 | 7.26 |
| | Weak | 5.58 | 8.45 | 6.49 | 5.13 | 7.19 | 6.98 | 6.46 | 5.41 | 7.17 |
| | Strong | 5.83 | 8.02 | 6.33 | 4.31 | 8.33 | 6.32 | 7.06 | 5.51 | 6.95 |
| Sub_6 | Normal | 4.53 | 7.94 | 7.96 | 6.39 | 5.97 | 4.69 | 6.70 | 5.06 | 6.74 |
| | Weak | 4.35 | 8.11 | 7.25 | 4.08 | 6.57 | 4.82 | 6.23 | 4.62 | 6.01 |
| | Strong | 4.47 | 8.19 | 7.03 | 4.59 | 7.94 | 6.24 | 6.04 | 5.40 | 4.60 |
| Ave. | Normal | 5.96 | 7.91 | 7.37 | 7.10 | 5.64 | 4.52 | 6.97 | 5.78 | 7.04 |
| | Weak | 5.79 | 8.29 | 7.59 | 5.73 | 6.43 | 5.19 | 6.44 | 5.67 | 7.13 |
| | Strong | 5.42 | 8.44 | 7.56 | 4.69 | 6.80 | 5.43 | 6.53 | 6.10 | 6.64 |

**Table 2.** Results of ANOVA at R. M. Shank.

| Variation Factor | | Sum of Sq. Diff. | DOF | Mean Sq. | F Val. | P Val. |
|---|---|---|---|---|---|---|
| $S_x$ | Be.Gr. | 17.554 | 2 | 8.777 | 8.528 | 0.003 |
| | With.Gr. | 15.438 | 15 | 1.029 | | |
| | Total | 32.992 | 17 | | | |
| $S_y$ | Be.Gr. | 4.247 | 2 | 2.123 | 1.739 | 0.209 |
| | With.Gr. | 18.311 | 15 | 1.221 | | |
| | Total | 22.558 | 17 | | | |
| $S_z$ | Be.Gr. | 2.656 | 2 | 1.328 | 1.317 | 0.297 |
| | With.Gr. | 15.125 | 15 | 1.008 | | |
| | Total | 17.781 | 17 | | | |

sults in **Table 2** show that for the $x$ coordinate, the singular values are significantly different between the three levels. The first singular values of R. M. Shank, therefore, are suggested to be an effective criterion to evaluate walking difficulty. That is, the first singular values from the $x$ coordinate acceleration of the restricted leg decreases with the increase of walking difficulty. The larger the first singular values are, the more serious the walking difficulty is.

The results in **Tables 1** and **2** show the possibility of evaluating walking disability using the singular values. The first singular values extracted from the acceleration data at R. M. Shank are plotted in a 3D space in **Fig. 5**. The singular values of the 4 trials of walking are plotted in different shapes and colors according to the 3 statuses. The average singular values of the 3 statuses are connected by black lines. **Fig. 5** shows that the first singular values are nearly separable in the 3D space according to the statuses. The line connecting the average values can be considered as severity line of walking difficulty. The visualization tool can be utilized in diagnosis or rehabilitation to assist walking difficulty evaluation.

Although statistically not significant, the singular values on the $x$ and $y$ coordinates at R. M. Shank increased on average with the increasing walking difficulty. The differences of the singular values between different coordinates, $S_x - S_y$ and $S_x - S_z$, were both in descending trends. The $S_x - S_y$ and $S_x - S_z$ plotted in **Figs. 6** and **7** for each subject illustrate descending trends with the increasing walking difficulty without exception. The differences is suggested to be effective in evaluating walking difficulty. On the other hand, a great inter-subject difference was also observed, which was caused by the difference in the dynamics of human walking. These results suggest that the $S_x - S_y$ and $S_x - S_z$ are effective in monitoring a person's walking difficulty (e.g., tracking the recovery of a patient during rehabilitation) while the inter-subject difference cannot be neglected when they are applied to evaluate walking difficulty between different persons.

Since the acceleration time-series data were normalized before performing the SW-SVD, the influence of magnitude difference caused by the restriction was excluded. The analysis results above therefore validate that the proposed SW-SVD is effective to extract features representing change patterns from time-series data. With the method in the previous study [27], although the singular values at R. M. Shank and L. M. Shank significantly decreased with the increasing walking difficulty, it was unable to identify which knee joint was restricted. By contrast, the singular values calculated with the SW-SVD

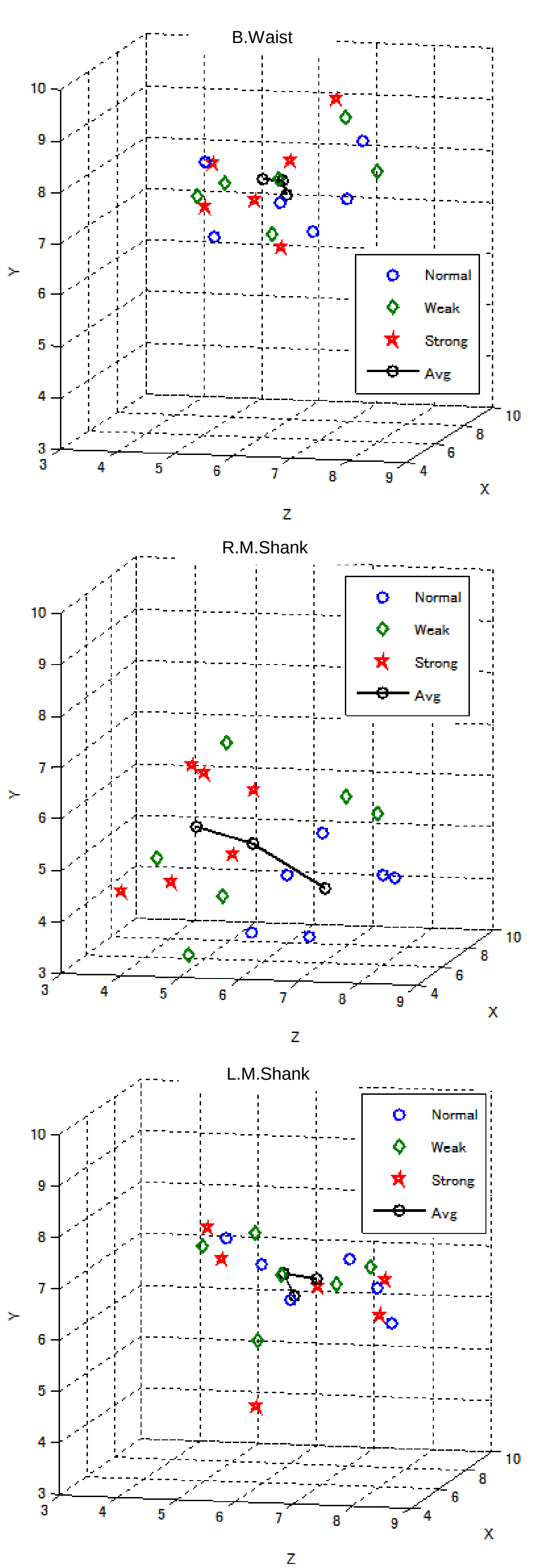


**Fig. 5.** Singular values plotted in 3D spaces. Shapes and colors indicate different statuses and their average.

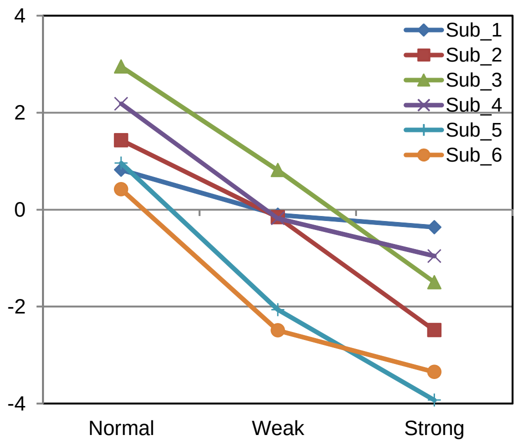


**Fig. 6.** $S_x - S_y$ at R. M. Shank.

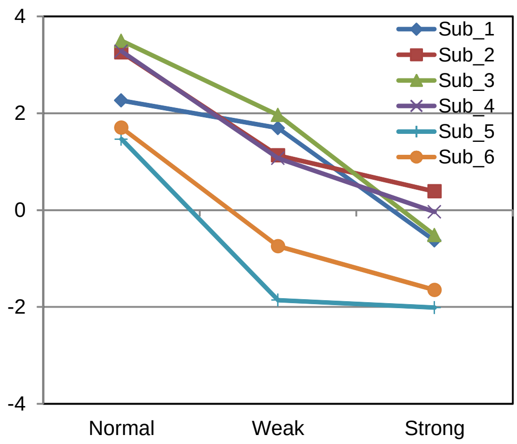


**Fig. 7.** $S_x - S_z$ at R. M. Shank.

only significantly decreased with the increasing walking difficulty at R. M. Shank on the restricted right leg. This suggests that the SW-SVD is more effective in extracting features from time-series data than the previous method.

## 5. Visualization of Walking Ability

The results in **Tables 1** and **2** and **Figs. 6** and **7** suggest that the first singular values are correlated with the level of walking difficulty and can be used as the criterion for the evaluation of walking disability. Objective measurements and correct interpretation of the measurement results can have a substantial impact on the recovery. A convenient assessment method is desired for those who rehabilitate at a hospital or exercise at home to keep them informed of their status anytime, and thus to stimulate the motivation to recover.

To provide a more understandable presentation of the data for the physical therapists and the patients to evaluate the recovery of walking ability by using the singular values calculated from the walking acceleration, we propose a visualization method to assist in the evaluation of walking difficulty. Although plotting the singular values in 3D

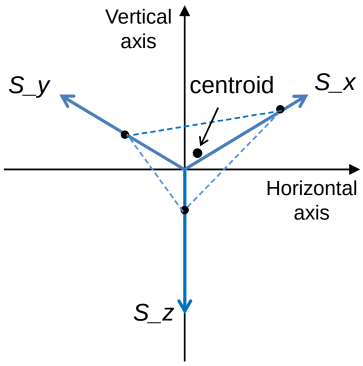


**Fig. 8.** Visualization triangle and its centroid. Dashed lines show the virtual triangle.

space like **Fig. 5** shows to some extent the visible information useful for comprehension, it may be still unfamiliar for the elderly. The acceleration are usually measured in 3 dimensions, the results of which are difficult to display on a flat screen emphasizing the representative features. In order to provide a more understandable presentation of the data for the physical therapists and the patients, we therefore design a display method to show the 3D singular values in 2 dimension while representing the features related to walking difficulty in an intuitive way.

As shown in **Fig. 8**, the singular values of the 3 dimensions are indicated by 3 vectors, the angles between which are 120°. The centroid of the triangle defined by the vertexes of the 3 vectors is used as the indicator to represent the features of the 3D singular values. By plotting the singular values calculated from the acceleration time-series in order of time, the centroid will represent the relationship between the singular values, and the trajectory of the centroid will make explicit the change patterns of the singular values according to the walking difficulty.

The trajectories of the centroids of the visualization triangles are shown in **Fig. 9**. Results of the first of the four trials of walking are plotted since results of the four trials are quite similar. Common change patterns can be observed intuitively in the results of all the six subjects. The centroids of the Normal status scatter along the diagonal stroke at an angle of approximately 45° to the horizontal. The centroids of the Weak status converge nearer to the point of origin than those of the Normal and Strong statuses. The centroids of the Strong status scatter along the horizontal. If ellipses are drawn to envelope the centroids of the three statuses, the ellipse of the Normal status is the biggest with its major axis being at an angle of approximately 45° to the horizontal. The ellipse of the Normal status is approximate to a circle with its center near to the point of origin. The ellipse of the Normal status has the smallest minor axis and its major axis is nearly parallel to the horizontal. Although the change patterns might be similar between different statuses of different subjects (e.g. Weak of Sub_5 and Normal of Sub_6), notable differences between the three statuses exist within one subject.

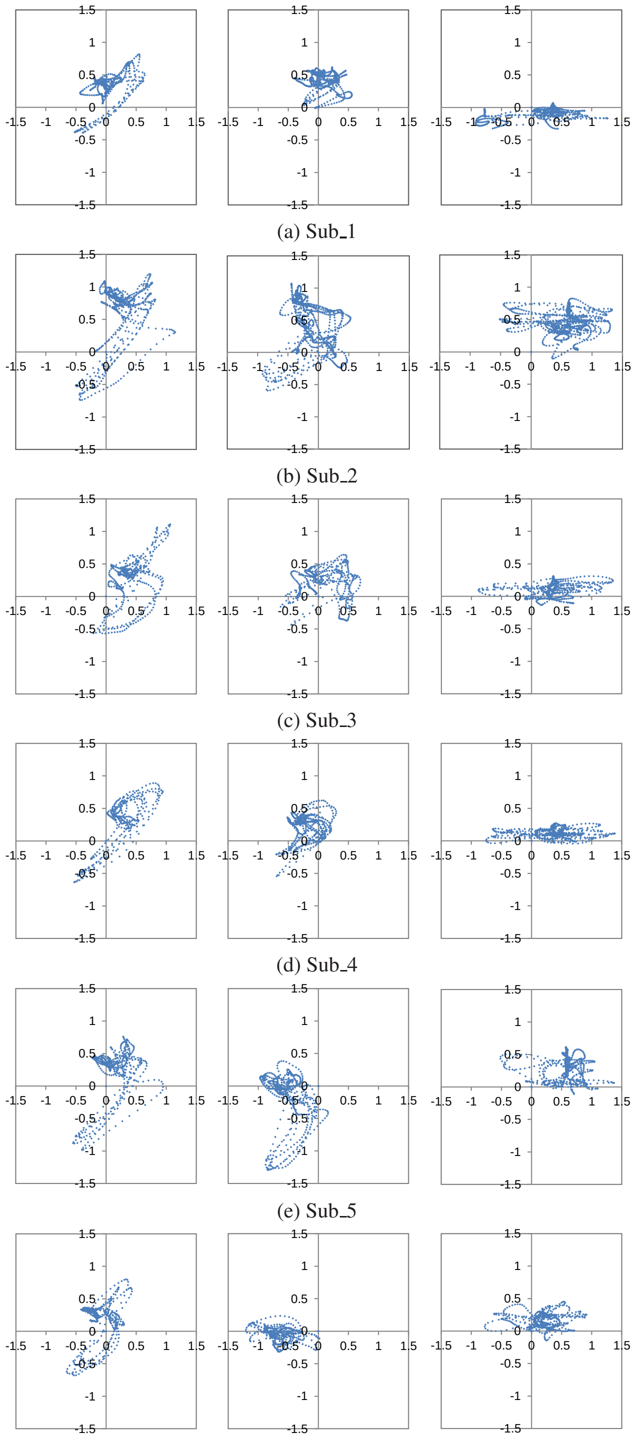

(a) Sub_1
(b) Sub_2
(c) Sub_3
(d) Sub_4
(e) Sub_5
(f) Sub_6

**Fig. 9.** The trajectories of the centroids the visualization triangles (left figure for Normal, middle figure for Weak, right figure for Strong).

## 6. Discussion

### 6.1. Performance of the SW-SVD

The SW-SVD for embodied knowledge extraction is proposed which performs SVD on the sliding window subsets of time-series data. The matrix for SVD is designed by overlapping the subsets of the time-series data. Different from the method of the previous study [27] that composed the matrix with data from different cycles of motion, the SW-SVD does not require segment preprocessing which is time-consuming and may affect the calculation results.

The SW-SVD is applied to evaluate the difficulty of walking with the singular values. The mean values of the first singular values listed in **Table 1** shows significant correlation with the walking statuses. Given that the acceleration time-series were normalized to exclude the effect of the magnitude of the acceleration caused by walking speed, these results suggested the effectiveness of the SW-SVD. In the previous study [27] which composed the matrix with data from segmented motion cycles, the singular values at R. M. Shank and L. M. Shank were significantly different between the walking difficulties. By contrast, the singular values calculated with the SW-SVD only significantly decreased with the increasing walking difficulty at R. M. Shank on the restricted right leg. Since the first singular value is a scalar measuring the impact of the first left singular vector, which is the most dominant pattern of the Hankel matrix, the correlation between the singular values and the walking statuses indicated that the impacts of the patterns change regularly according to the walking difficulties.

## 6.2. Practicality

Biological signals, most of which are time-series data, are being widely measured and analyzed in the field of health care. The singular values and the singular vectors can provide a new perspective to look into the time-series data of motions. As a basic ability required for independent daily life, walking has been studied extensively and there have been varied approaches to handle walking analysis, ranging from kinematic models to gait feature analysis such as stride length and gait cycle. Walking with different disabilities has a similar pattern or characteristic. The strength of the most dominant characteristic, which is represented by the first singular vector, is significantly different according to the levels of walking difficulties. **Figs. 6** and **7** suggest the practicality of the singular values as a criterion to evaluate walking ability. The singular values can be utilized as a criterion for the evaluation of recovery in walking rehabilitation.

The visualization method was further proposed to show singular values in an easily understandable way for the patients and the physical therapist. The visualization of analytical results is critical in practical use for a person without academic background to get informed [36, 37]. A visualization triangle, defined by the singular values from the walking acceleration, is proposed as a visualization tool to assist the evaluation of the walking disability. The physical therapist and the patient can intuitively evaluate the recovery progress with the trajectory change of the centroids of the triangles defined by the singular values. The gradual pattern changes is visually indicated to be from diagonal distribution along the stroke at an angle of approximately 45 to converging to the point of origin, and to flatting along the horizontal with the increase of walking diffculty. The kind of correlation between the patterns and disabilities provides a tool available for the patients in rehabilitation to keep informed of their recovery.

## 6.3. Future Work

The proposed SW-SVD was applied to walking evaluation by analyzing the time-series of acceleration. Besides the acceleration data analyzed in this study, it can also be applied to analyze other time-series data such as angular velocity and position. A better evaluation may be achieved by analyzing multimodal kinesiological data. The parameters, $n$ and $m$, that determine the Hankel matrix in the SW-SVD need to be further discussed. The current calculation with $n = 10$, $m = 10$ has shown the effectiveness and applicable prospect of the SW-SVD. The appropriate value of $n$ and $m$ might be related with the sampling rate of measurement and the speed and cycle of the motion. The SW-SVD is a method to investigate the fundamental features of time-series data. Superior features important for motion evaluation, such as symmetry/asymmetry [38] and cycle characteristics [39], can be studied based on the fundamental features of singular values and singular vectors. We will further investigate the features extracted by SW-SVD by comparing it to other time-series analysis methods in our future work.

Only the first singular values were considered in the current analysis to evaluate the walking difficulty. The detailed gait pattern change with walking difficulty can be extracted by the left singular vectors. The other singular values and the singular vectors may also contain information significantly associated with the motion patterns. Future work will study the usefulness of the other components, and experiments of motions besides walking will be conducted to further validate the SW-SVD.

**Acknowledgements**

This work was partially supported by JSPS KAKENHI Grant Numbers JP15H03951, JP16K01539, JP16K12503, and the Canon Foundation.

**References:**

[1] A. Kendon, "Gesture: Visible Action as Utterance," Cambridge University Press, Cambridge, Sep. 2004.

[2] A. L. Hubbard, S. M. Wilson, D. E. Callan, and M. Dapretto, "Giving speech a hand: gesture modulates activity in auditory cortex during speech perception," Human Brain Mapping, Vol.30, No.3, pp. 1028-1037, Mar. 2009.

[3] L. E. Holt and S. L. Beilock, "Expertise and its embodiment: Examining the impact of sensorimotor skill expertise on the representation of action-related text," Psychonomic Bulletin& Review, Vol.13, No.4, pp. 694-701, Aug. 2006.

[4] D. C. Spencer, "Habit(us), body techniques and body callusing: An ethnography of mixed martial arts," Body & Society, Vol.15, No.4, pp. 119-143, Dec. 2009.

[5] S. Furuya, R. Osu, and H. Kinoshita, "Effective utilization of gravity during arm downswing in keystroke by expert pianists," Neuroscience, Vol.164, No.2, pp. 822-831, Dec. 2009.

[6] D. Gafurov, E. Snekkenes, and P. Bours, "Spoof Attacks on Gait Authentication System," IEEE Trans. on Information Forensics and Security, Vol.2, No.3, pp. 491-502, Sep. 2007.

[7] T. Takeda, K. Kuramoto, S. Kobashi, and Y. Hata, "A challenge to biometrics by sole pressure while walking," Proc. 2011 IEEE Int. Conf. on Fuzzy Systems, pp. 1430-1435, June 2011.

[8] D. M. Wolpert, R. C. Miall, and M. Kawato, "Internal models in the cerebellum," Trends in Cognitive Sciences, Vol.2, No.9, pp. 338-347, Sep. 1998.

[9] H. Imamizu and M. Kawato, "Cerebellar internal models: Implications for the dexterous use of tools," The Cerebellum, Vol.11, No.2, pp. 325-335, Jun. 2012.

[10] T. M. Hall, F. de Carvalho, and A. Jackson, "A Common Structure Underlies Low-Frequency Cortical Dynamics in Movement, Sleep, and Sedation," Neuron, Vol.83, No.5, pp. 1185-1199, Sep. 2014.

[11] Y. Nakayama, K. Kudo, and T. Ohtsuki, "Variability and fluctuation in running gait cycle of trained runners and non-runners," Gait & Posture, Vol.31, No.3, pp. 331-335, Mar. 2010.

[12] R. Williamson, and B. J. Andrews, "Gait event detection for FES using accelerometers and supervised machine learning," IEEE Trans. on Rehabilitation Engineering, Vol.8, No.3, pp. 312-319, Sep. 2000.

[13] T. Pylvanainen, "Accelerometer based gesture recognition using continuous HMMs," in Pattern Recognition and Image Analysis, New York: Springer Berlin/Heidelberg, pp. 639-646, Jun. 2005.

[14] J. K. Aggarwal and M. S. Ryoo, "Human activity analysis: A review," ACM Computing Surveys, Vol.43, No.3, Article 16, 43 pages, 2011.

[15] S. Mitra and T. Acharya, "Gesture recognition: A survey," IEEE Trans. on Systems, Man, and Cybernetics, Part C, Vol.37, No.3, pp. 311-324, May 2007.

[16] A. D. Wilson and A. F. Bobick, "Parametric hidden Markov models for gesture recognition," IEEE Trans. on Pattern Analysis and Machine Intelligence, Vol.21, No.9, pp. 884-900, Sep 1999.

[17] J. F. Lichtenauer, E. A. Hendriks, and M. J. T. Reinders, "Sign language recognition by combining statistical DTW and independent classification," IEEE Trans. on Pattern Analysis and Machine Intelligence, Vol.30, No.11, pp. 2040-2046, Nov. 2008.

[18] M. V. Lamar, M. S. Bhuiyan, and A. Iwata, "Hand gesture recognition using T-CombNET: A new neural network model," IEICE Trans. on Information and Systems, Vol.E83-D, No.11, pp. 1986-1995, Nov. 2000.

[19] T. E. Jerde, J. F. Soechting, and M. Flanders, "Biological constraints simplify the recognition of hand shapes," IEEE Trans. on Biomedical Engineering, Vol.50, No.2, pp. 265-269, Feb. 2003.

[20] A. Daffertshofer, C. J. Lamoth, O. G. Meijer, and P. J. Beek, "PCA in studying coordination and variability: A tutorial," Clinical Biomechanics, Vol.19, No.4, pp. 415-428, May 2004.

[21] T. L. Jakobsen, M. Christensen, S. S. Christensen, M. Olsen, and T. Bandholm, "Reliability of knee joint range of motion and circumference measurements after total knee arthroplasty: Does tester experience matter?," Physiotherapy Research Int., Vol.15, No.3, pp. 126-134, Sep. 2010.

[22] M. E. Wall, A. Rechtsteiner, and L. M. Rocha, "Singular value decomposition and principal component analysis," in D. P. Berrar, W. Dubitzky, and M. Granzow (eds.), A Practical Approach to Microarray Data Analysis, pp. 91-109, Kluwer, Norwell, MA 2003.

[23] D. B. Skillicorn, "Understanding Complex Datasets: Data Mining with Matrix Decompositions," Florida, USA: Chapman and Hall/CRC, May 2007.

[24] H. Nakanishi, S. Kanata, H. Hattori, T. Sawaragi, and Y. Horiguchi, "Extraction of coordinative structures of motions by segmentation using singular spectrum transformation," J. Adv. Comput. Intell. Intell. Inform., Vol.15, No.8, pp. 1019-1029, Oct. 2011.

[25] A. Cavallo and P. Falco, "Online Segmentation and Classification of Manipulation Actions From the Observation of Kinetostatic Data," IEEE Trans. on Human-Machine Systems, Vol.44, No.2, pp.256-269, Apr. 2014.

[26] I. Hayashi, Y. Jiang, and S. Y. Wang, "Acquisition of Embodied Knowledge on Gesture Motion by Singular Spectrum Analysis," J. Adv. Comput. Intell. Intell. Inform., Vol.15, No.8, pp. 1011-1018, 2011.

[27] Y. Jiang, I. Hayashi, and S. Wang, "Knowledge acquisition method based on singular value decomposition for human motion analysis," IEEE Trans. on Knowledge and Data Engineering, Vol.26, No.12, pp.3038-3050, Dec. 2014.

[28] A. Pantelopoulos and N. G. Bourbakis, "A survey on wearable sensor-based systems for health monitoring and prognosis," IEEE Trans. on Systems, Man, and Cybernetics, Part C: Applications and Reviews, Vol.40, No.1, pp.1-12, Jan. 2010.

[29] S. Cheng, K. Tom, L. Thomas, and M. Pecht, "A wireless sensor system for prognostics and health management," IEEE Sensors J., Vol.10, No.4, pp.856-862, Apr. 2010.

[30] J. J. Kavanagh and H. B. Menz, "Accelerometry: a technique for quantifying movement patterns during walking," Gait & Posture, Vol.28, No.1, pp.1-15, Jul. 2008.

[31] H. Lau and K. Tong, "The reliability of using accelerometer and gyroscope for gait event identification on persons with dropped foot," Gait and Posture, Vol.27, No.2, pp. 248-257, Feb. 2008.

[32] M. Yoneyama, Y. Kurihara, K. Watanabe, and H. Mitoma, "Accelerometry-based gait analysis and its application to parkinson's disease assessment - part 2 : a new measure for quantifying walking behavior," IEEE Trans. on Neural Systems and Rehabilitation Engineering, Vol.21, No.6, pp. 999-1005, Nov. 2013.

[33] M. Iosa, G. Morone, A. Fusco, L. Pratesi, M. Bragoni, P. Coiro, M. Multari, V. Venturiero, D. De Angelis, and S. Paolucci, "Effects of walking endurance reduction on gait stability in patients with stroke," Stroke Research and Treatment, article ID 810415, 6 pages, 2012.

[34] O. Chuy, Y. Hirata, and K. Kosuge, "A new control approach for a robotic walking support system in adapting user characteristics," IEEE Trans. on Systems, Man, and Cybernetics, Part C: Applications and Reviews, Vol.36, No.6, pp. 725-733, Nov. 2006.

[35] K. Wakita, J. Huang, P. Di, K. Sekiyama, and T. Fukuda, "Human-walking-intention-based motion control of an omnidirectional-type cane robot," IEEE/ASME Trans. on Mechatronics, Vol.18, No.1, pp. 285-296, Feb. 2013.

[36] C. B. Redd and S. J. M. Bamberg, "A wireless sensory feedback device for real-time gait feedback and training," IEEE/ASME Trans. on Mechatronics, Vol.17, No.3, pp. 425-433, Jun. 2012.

[37] D. Piovesan, P. Morasso, P. Giannoni, and M. Casadio, "Arm stiffness during assisted movement after stroke: the influence of visual feedback and training," IEEE Trans. on Neural Systems and Rehabilitation Engineering, Vol.21, No.3, pp. 454-465, May 2013.

[38] M. Yoneyama, "Visualising gait symmetry/asymmetry from acceleration data," Computer Methods in Biomechanics and Biomedical Engineering, Vol.18, No.9, pp. 923-930, Jul. 2015.

[39] R. Moe-Nilssen and J. L. Helbostad, "Estimation of gait cycle characteristics by trunk accelerometry," J. of Biomechanics, Vol.37, No.1, pp. 121-126, Jan. 2004.



**Name:**
Yinlai Jiang

**Affiliation:**
Brain Science Inspired Life Support Research Center, The University of Electro-Communications

**Address:**
185 Miyanoguchi, Tosayamada, Kami, Kochi 782-8502, Japan


**Brief Biographical History:**

2008 Received Ph.D. in Engineering, Kochi University of Technology
2008-2012 Research Associate, Kochi University of Technology
2012-2014 Kochi University of Technology
2014- Associate Professor, The University of Electro-Communications

**Membership in Academic Societies:**

- The Institute of Electrical and Electronic Engineers (IEEE)
- Japan Society for Fuzzy Theory and Intelligent Informatics (SOFT)
- The Robotics Society of Japan
- Japanese Society for Medical Engineering

**Name:**
Isao Hayashi

**Affiliation:**
Professor, Graduate School of Informatics, Kansai University

**Address:**
2-1-1 Ryozenji-cho, Takatsuki, Osaka 569-1095, Japan

**Brief Biographical History:**
1981-1983 Sharp Corporation
1987-1993 Panasonic Corporation
1993-2004 Hannan University
2004- Kansai University

**Membership in Academic Societies:**
- International Fuzzy Systems Association (IFSA)
- The Institute of Electrical and Electronics Engineers (IEEE)
- Japan Society for Fuzzy Theory and Intelligent Informatics (SOFT)
- Japanese Neural Network Society (JNNS)

**Name:**
Shuoyu Wang

**Affiliation:**
Department of Intelligent Mechanical Systems Engineering, Kochi University of Technology

**Address:**
185 Miyanoguchi, Tosayamada, Kami, Kochi 782-8502, Japan

**Brief Biographical History:**
1993 Received Ph.D. in Electrical Engineering, Hokkaido University
1993-1997 Assistant Professor, Yamagata University
1997-2002 Associate Professor, Kochi University of Technology
2002- Professor, Kochi University of Technology

**Membership in Academic Societies:**
- The Institute of Electrical and Electronic Engineers (IEEE)
- Japan Society for Fuzzy Theory and Intelligent Informatics (SOFT)
- The Robotics Society of Japan
- The Japan Society of Mechanical Engineering
- The Society of Life Support Engineering
- Japanese Society for Medical and Biological Engineering

**Name:**
Kenji Ishida

**Affiliation:**
Kurihara Central Hospital

**Address:**
Kurihara, Miyagi 987-2205, Japan

**Brief Biographical History:**
1987 Received Medical Doctor degree in Kochi Medical School
2003 Received Ph.D. in Medicine, Kochi Medical School
2003-2007 Assistant Professor, Department of Kochi Medical School, Kochi University
2007-2014 Associate Professor, Department of Kochi Medical School, Kochi University
2014- Professor, Kurihara Central Hospital

**Membership in Academic Societies:**
- The Japanese Association of Rehabilitation Medicine
- Japan College of Rheumatology
- The Society of Life Support Engineering
- The Japanese Orthopaedic Association
- Japanese Society of Electroencephalography and Electromyography